Aerosol fluxes in the breaker zone of the Gulf of Gdańsk

OCEANOLOGIA, No. 35
pp. 13–25, 1993.
PL ISSN 0078–3234

Aerosol
Flux
Breaker zone
Lidar

TYMON ZIELIŃSKI
Institute of Oceanography,
University of Gdańsk,
Gdynia

Manuscript received December 21, 1993, in final form May 13, 1994.

Abstract

This article presents the results of calculations of concentrations, fluxes and velocities of aerosol particles produced in the process of wave breaking. The calculations were carried out using experimental data collected during lidar-based investigations of marine aerosols above the breaker zone of the Gulf of Gdańsk. The sounding profiles obtained were used to determine aerosol concentration and size distribution functions on which the flux and velocity calculations were based. The comparative method introduced by Potter (1987) was used to derive these parameters.

1. Introduction

Oceanic processes have traditionally been investigated by instrumental sampling *in situ*, yielding quantitative measurements that are discontinuous in both space and time. The rapid development of quantum electronics has permitted the introduction of efficient remote-sensing techniques for air and sea based on applied laser spectroscopy. These active techniques make it possible to do quick and simultaneous measurements of optical parameters of an entire ensemble of aerosol particles over a distance of many kilometres and under various hydrometeorological conditions.

Lidar methods play a special role in marine aerosol investigations (Zuyev and Naats, 1983; Piskozub, 1991). Given the dynamic parameters of the atmosphere and using a multifrequency lidar, the height profile and aerosol size distribution can be determined for various areas, including breaker zones.

Breaking waves directly influence both current generation and turbulence in the water body, and therefore influence all phenomena that depend on the mixing of oceanic upper layers (Mestayer, 1990). Such waves are, moreover, responsible for disrupting the chemical and organic surface films,

and produce a great number of air bubbles, which are entrained in the water body. This causes the sea–to–air exchange of gases, moisture and dry nuclei, which must be described by relations other than those used to describe surface transfer (Mestayer, 1990). The differences in the total number of particles produced in the breaker zone compared to the open sea can be easily detected using lidar, whose sensing distance is greater than the extent of the breaker zone.

This article presents the results of lidar-based investigations focused on the breaker zone of the Gulf of Gdańsk at Hel.

2. Apparatus and methods

The FLS–12 lidar system used for the measurements is a tunable laser system designed for remote sensing the aquatic environment and atmosphere in the UV–VIS spectrum. It is owned by the Institute of Oceanology, Polish Academy of Sciences, Sopot.

The UV pumping source for the dye laser is an XeCl (308 nm) excimer laser. The beam divergence of 1 mrad makes it possible to use the excimer laser both for pumping and as a separate source of the lidar sounding signal. The energy of a single impulse may reach 70 mJ. The radiance scattered by the target particles is collected by an optical system which includes a telescope and a polychromator. This telescope is of the hermetically sealed Cassegrian type (280 mm receiver diameter) with a conforming grating polychromator for the 250–800 nm (450 lines/mm) spectral range. The signal returning from various ranging distances is registered by the separate channels of a multichannel photoreceiver. More detailed information about the FLS–12 can be found in Zieliński *et al.* (1992).

Visible light of wavelengths $\lambda_1 = 443$ nm, $\lambda_2 = 445$ nm, $\lambda_3 = 450$ nm, $\lambda_4 = 562$ nm, $\lambda_5 = 566$ nm was used for the measurements. Radiation was generated by a dye laser employing Coumarin 120 (λ_1, λ_2 and λ_3) and Rhodamine 110 (λ_4 and λ_5) dye solutions. The useful part of the optical paths lay between 60 and 420 m. Altitudes up to 60 m were sounded. The scattered signal was registered every 50 ns, that is, every 7.5 m on the optical path. Signal values averaged after 20 pulses for all wavelengths served as the basis for determining the size distribution of aerosol particles, their total concentration as well as particle fluxes at given altitudes. The comparative method of solving the lidar problem (Potter, 1987) was used to determine the optical parameters of the aerosol, especially its extinction coefficient α (z, λ) at every point on the optical path. The extinction coefficient α_{ij} at point z_i and wavelength λ_j is described by

$$\alpha_{ij}(z_i, \lambda_j) = \int_{r_1}^{r_2} Q(r, \lambda_j)\, s(r, z_i)\, dr, \tag{1}$$

where r is the particle radius, $s(r)$ is the total geometric cross-section distribution of aerosol particles per unit volume, and $Q(r, \lambda_j)$ is a dimensionless Mie theory extinction coefficient. It was assumed that the ensemble of marine aerosol particles consisted of non-absorbing spherical water droplets, and that the function $s(r)$ takes the form corresponding to the power law for size distribution:

$$s(r) = ar^2 \exp(-br), \tag{2}$$

where $a, b > 0$ are distribution parameters. Non-linear minimization was used to determine the values of the distribution parameters a and b best fitting formula (1). These coefficients determine the size distribution function and aerosol concentration at particular altitudes for $r \epsilon [0.2\,\mu\text{m}, 5\,\mu\text{m}]$ as follows:

$$N_c(h) = (a/b) \exp(-0.2b) \tag{3}$$

and

$$N_r(h) = N_c(h) f(r), \tag{4}$$

where $f(r) = b \exp(-br)$ and $\int f(r)dr = 1$.

Such a range of sizes was determined not only by the lidar's spectral resolution, but also by the occurrence of large droplets ($r > 5\,\mu\text{m}$) in the atmosphere (Garbalewski, 1983a,b). For more detailed information about the computing steps, see Zieliński *et al.* (1992).

Aerosol particle concentrations at altitude $H = 0\,\text{m}$ were obtained from

$$N^o(H) = N(H) \exp(\gamma H), \tag{5}$$

where $\gamma\,[m^{-1}]$ is a coefficient, the value of which depends on particle size. This dependence of coefficient γ on particle size is presented in Tab. 1 (Cartney, 1976).

Table 1. Dependence of coefficient γ on particle radius

r [μm]	γ [m^{-1}]
0.5	3×10^{-4}
1.0	3.2×10^{-4}
2.5	5×10^{-4}
5.0	11×10^{-4}

3. Area and conditions of the investigations

The field measurements were carried out in November 1992. The boundary layer of the atmosphere above the breaker zone in the Gulf of Gdańsk was investigated from a point located 60 m offshore at Hel (see Fig. 1):

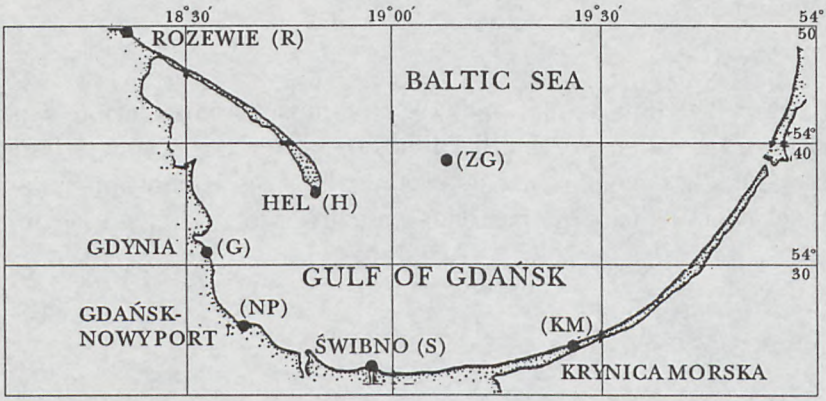

Fig. 1. Location of the measurement area

The air temperature T varied from 275 K to 280 K, the air pressure p from 990 hPa to 1002 hPa and the relative humidity RH from 80 % to 97 %. The wind velocity u_{10} at altitude $H = 10$ m ranged from 5 m s^{-1} to 19 m s^{-1}. The wind direction was S and SW. The slightly sloping sea bottom in the study area is smooth and consists of sand. An area 180 m offshore was investigated. This distance was selected on the basis of a formula describing the breaker zone under certain hydrometeorological conditions (Thurman, 1982):

$$D = 1.3\,h, \tag{6}$$

where D is depth, and h denotes wave height, a figure which depends on the wind speed u_{10} and wind direction. The maximum wave height under the hydrometeorological conditions obtaining during the investigations was *ca.* $h = 2$ m (Robakiewicz, 1991).

4. Results and discussion

The mean aerosol number concentration N per unit volume was determined at an altitude of 10 m for various wind speeds u_{10}. Fig. 2 shows the results of these calculations.

The variations in the calculated mass concentrations at the sea surface ($H = 0$ m) with particle sizes at a selected wind speed of $u_{10} = 19$ m s^{-1} are shown in Fig. 3.

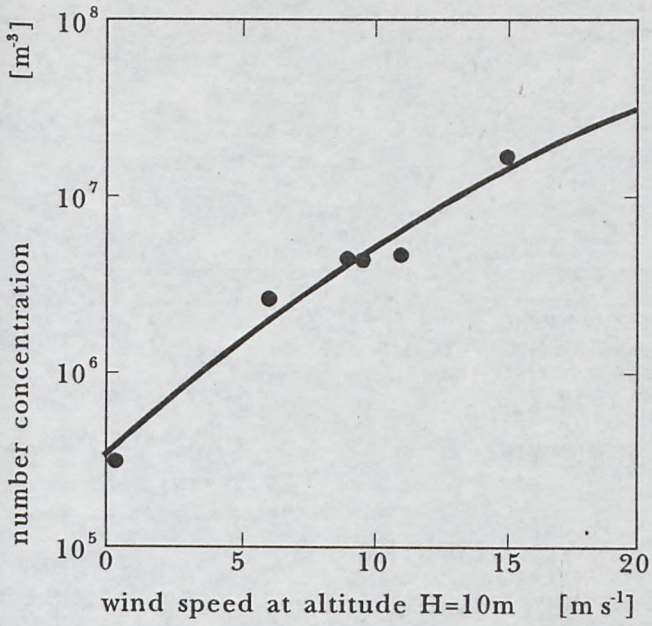

Fig. 2. Mean aerosol number concentration as a function of wind speed

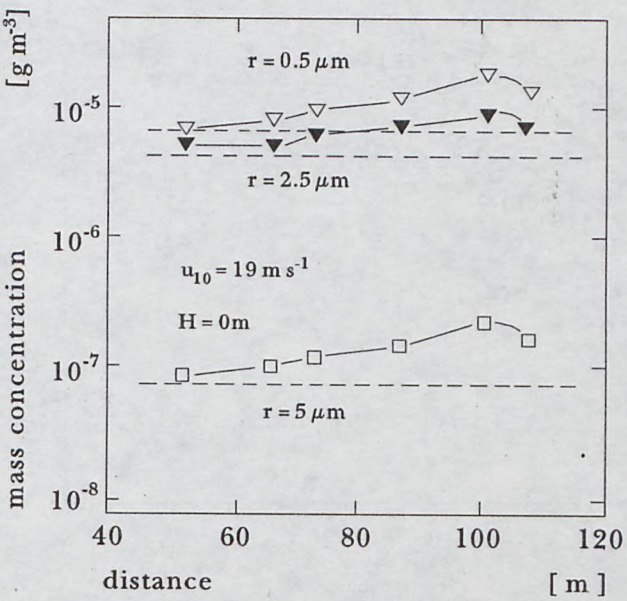

Fig. 3. Dependence of calculated mass concentrations at the sea surface ($H = 0\,\mathrm{m}$) of various particles and at a selected wind speed $u_{10} = 19\ \mathrm{m\ s^{-1}}$

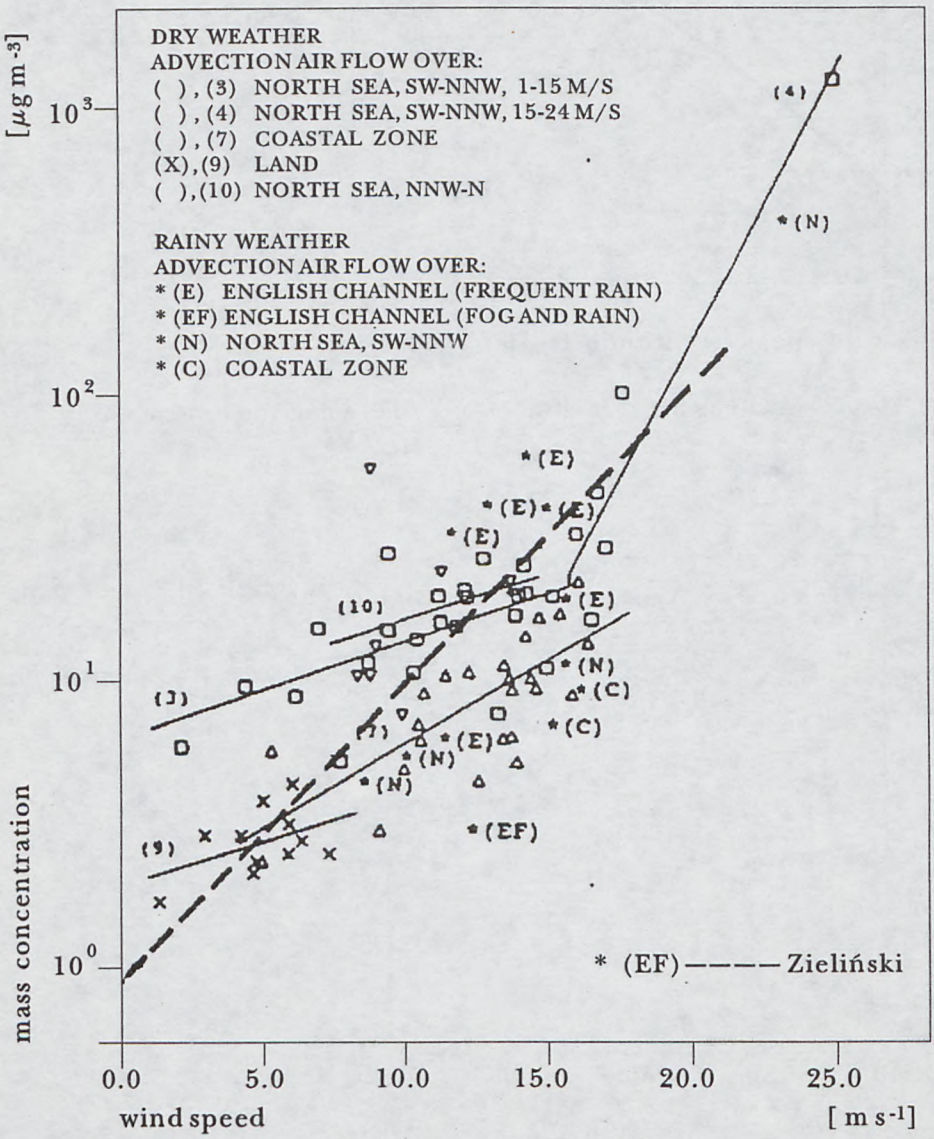

Fig. 4. Comparison of mass concentrations at various wind speeds obtained by Marks and Monahan (1988) and Zieliński *et al.* (1992)

Fig. 3 reveals that the mass concentrations of all particles are higher in the breaker zone than on the open sea (straight, horizontal lines). Furthermore, these results show a correlation with the results obtained by Marks (1987) for the North Atlantic and Greenland Sea, and by Marks and Monahan (1988) for the North Sea. The latter set of results is compared with my own (Zieliński *et al.*, 1992) in Fig. 4.

The dependence of mass concentration on altitude for three sizes of particles at a selected wind speed is shown in Fig. 5.

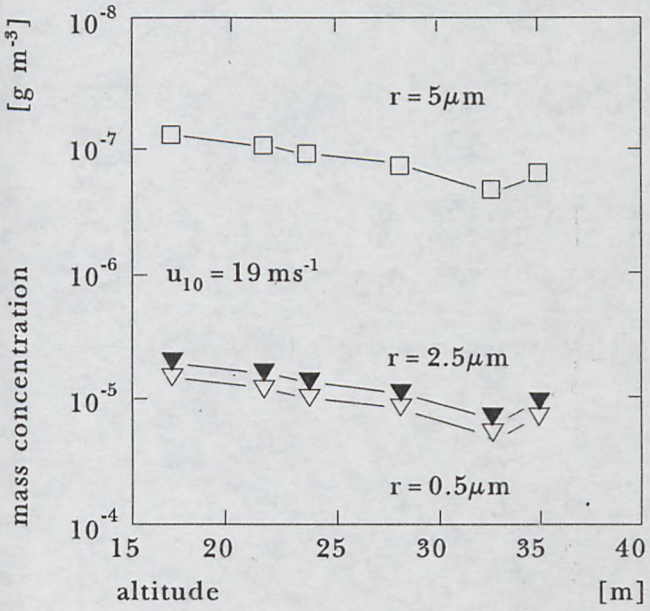

Fig. 5. Calculated mass concentration at a sellected wind speed of $u_{10} = 19$ m s^{-1} of various particles at various altitudes

Fig. 5 shows that the higher the altitude, the smaller the mass concentration is for all particles. This is a well documented fact. The minimum occurring at an altitude of about 30 m may have been caused either by measurement error or by the fact that at the time of the experiment, the temperature of the sea water was higher than that of the air. Particles produced and released into the air altered in size as a result of temperature changes and were removed from the air. Temperature equilibrium could have occurred at an altitude of about 30 m. This suggestion is supported by the lifetime of a particle in the air. In addition, this inversion might have been caused by an inflow of man-made aerosol.

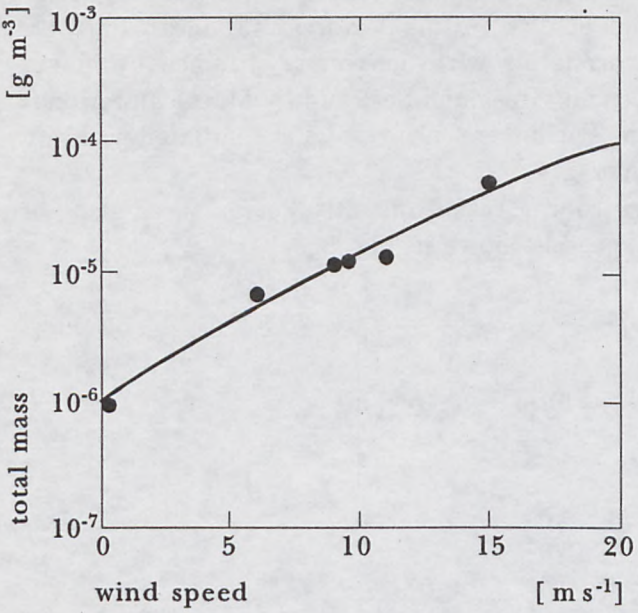

Fig. 6. Dependence of calculated total aerosol mass on wind speed

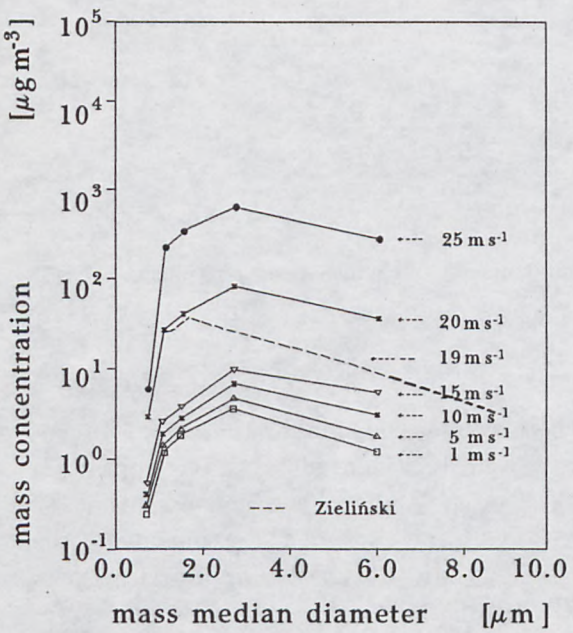

Fig. 7. Comparison of the total mass of aerosols obtained experimentally for the Gulf of Gdańsk with that obtained for the North Sea by Marks and Monahan (1988)

Fig. 6 shows the total mass of aerosols as a function of wind velocity u_{10}.

The results shown in Fig. 6 correlate with those obtained by Marks and Monahan (1988) for the North Sea by means of high volume stage impactors. Fig. 7 compares mass concentration *vs.* mass median diameter plots obtained by Marks and Monahan (1988) for the North Sea and by Zieliński *et al.* (1992) for the Gulf of Gdańsk.

The slightly different curve shapes can be explained by the fact that the Baltic Sea has a lower salinity and a more polluted surface than the North Sea. The masses obtained were used to determine mean fluxes. The mean fluxes of particles produced were derived from

$$F = v_D M, \tag{7}$$

where v_D is the deposition velocity. The deposition velocities are given by the expression shown below, derived by Carruthers and Choularton (1986) for near-natural conditions:

$$v_D = \frac{v_t}{1 - \exp[-v_t / c_D u]}, \tag{8}$$

where c_D and u are the drag coefficient and wind velocity at the measurement altitude respectively. Values of c_D for a given wind speed u were calculated using the following expression from Large and Ponds (1982):

$$\begin{aligned} c_D &= 1.14 \times 10^{-3} \quad u < 10\,\mathrm{m\,s^{-1}} \\ c_D &= (0.49 + 0.065\,u) \times 10^{-3} \quad u > 10\,\mathrm{m\,s^{-1}}. \end{aligned} \tag{9}$$

The results of these calculations are shown in Fig. 8.

The obtained mean flux versus wind speed plot correlates with that obtained by Garbalewski (1983a,b). Using the results of calculations carried out for mass concentrations and fluxes the particle velocities were worked out from

$$F = c\,v. \tag{10}$$

Fig. 9 shows the variations in velocity of particles of various radii at the sea surface ($H = 0\,\mathrm{m}$) for a selected wind speed of $u_{10} = 19\ \mathrm{m\ s^{-1}}$.

The shape of the curves in Fig. 9 are similar to the shapes of the mass concentration curves in Fig. 3.

Fig. 10 shows the velocities of particles of radius $r = 5\,\mu\mathrm{m}$ calculated for two wind speeds u_{10}.

The nature of the curves was identical for other particle sizes and corresponds to the distribution of mass concentration with altitude. The typical shapes of the scattered signals at wind speeds $u_{10} = 6\ \mathrm{m\ s^{-1}}$ and $u_{10} = 19\ \mathrm{m\ s^{-1}}$ are shown in Fig. 11.

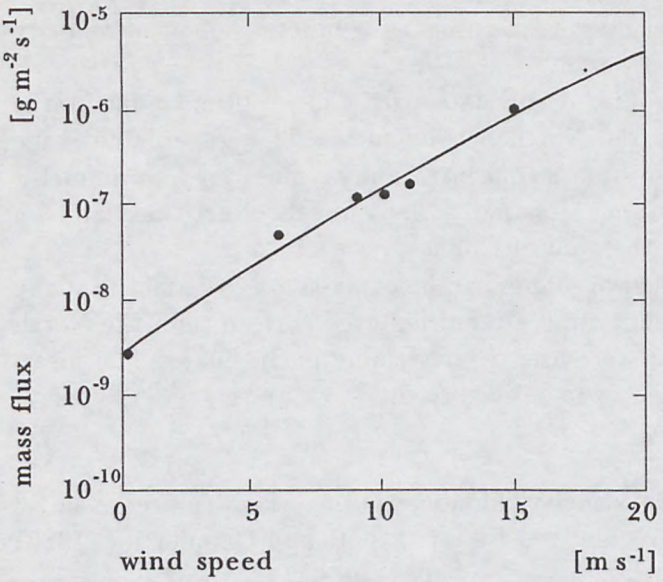

Fig. 8. Dependence of mean aerosol flux on wind speed

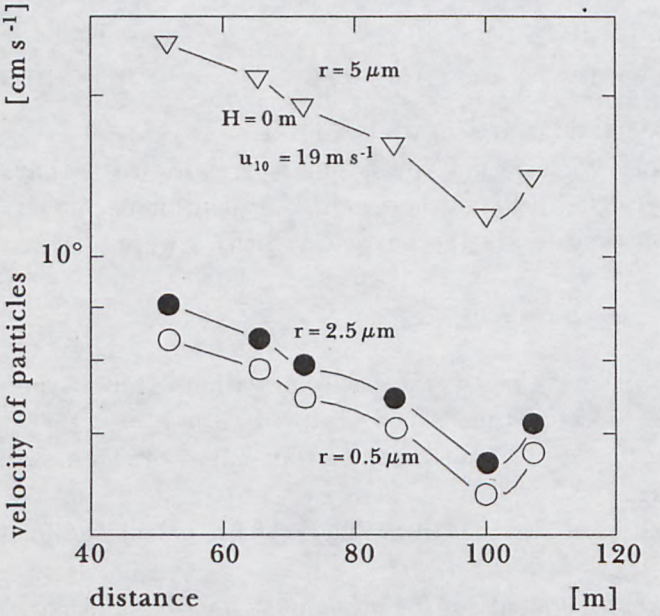

Fig. 9. The variations in velocity of particles of various radii at sea level ($H = 0\,\mathrm{m}$) for a selected wind speed of $u_{10} = 19\ \mathrm{m\ s^{-1}}$

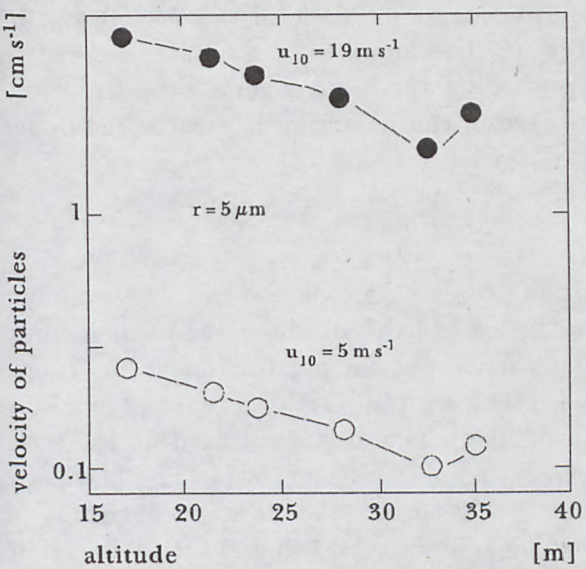

Fig. 10. Velocities of particles of radius $r = 5\ \mu$m at two wind speeds $u_{10} = 5$ m s^{-1} and $u_{10} = 19$ m s^{-1} at various altitudes

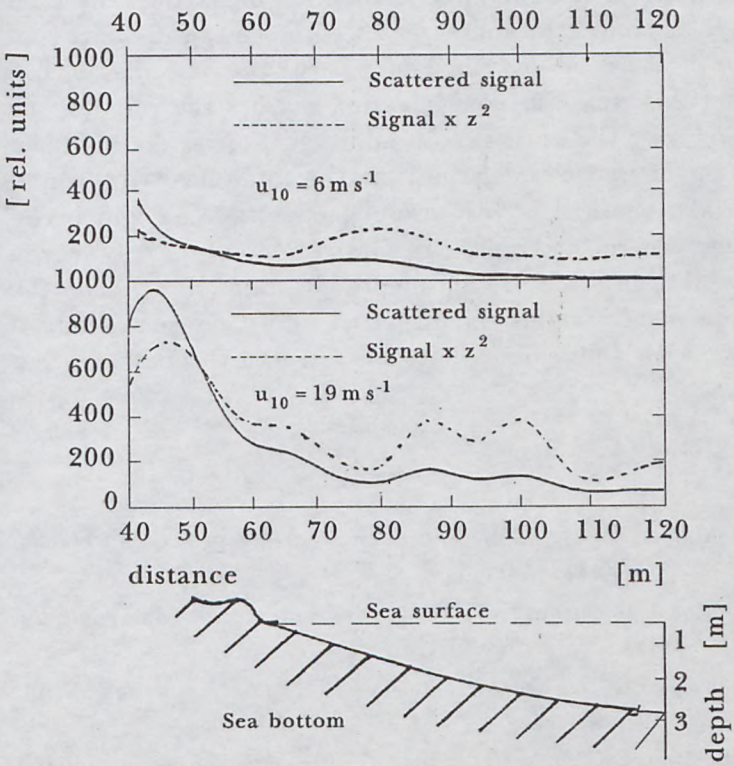

Fig. 11. Examples of backscattered signal *vs.* sounding distance and water depth plots for wind speeds $u_{10} = 6$ m s^{-1} and 19 m s^{-1}

Moreover, this figure shows the shape and slope of the sea bottom in the area which, on the basis of eq. (6) was found to be a breaker zone. The backscattered signal is clearly greater for the breaker zone (60 m from the lidar system). In this zone, the aerosol concentration is greater than over land or the open sea (see also Fig. 3).

5. Conclusions

This paper presents the results of investigations aimed at determining the exchange processes between the sea and the air above the breaker zone. The results of the investigations carried out for particles of radius range $r \epsilon (0.2, 5\,\mu\text{m})$ correlate with the results for the North and Greenland Seas (Marks 1987; Marks and Monahan, 1988). The results obtained for the total mass confirm that eq. (2), which was applied to the calculations, had been chosen correctly. The measurements showed that the mass concentration of the aerosols produced in the breaker zone increases linearly with the wind velocity u_{10}. The results did not show any perturbations in the function's shape. The size distribution function changes its shape with wind velocity u_{10} and in all cases displays maximum concentration of particles of $1\,\mu$m radius (see Fig. 7). This concentration increases with sensing distance and reaches a maximum in the zone described by eq. (6) *i.e.* at a distance of about 100 m. Beyond this zone, the concentration reaches the value of the particle concentration over the open sea. In addition, the results obtained for the mean fluxes of the particles derived from the total mass were found to be correct. The lidar method is very useful in determining and investigating coastal zones, where the transfer of mass, momentum and energy also depends on sea bottom structure and depth. In order to describe the above-mentioned dependence further, investigations must be carried out of various breaker zones with different sea bottoms (structure and slope) and during various seasons.

References

Carruthers D. J., Choularton T. C., 1986, *The microstructure of hill cap clouds*, Quart. J. R. Met. Soc., 1/2, 113–129.

Cartney E. J., 1976, *Optics of the atmosphere. Scattering by molecules and particles*, J. Wiley (ed.), New York.

Garbalewski C., 1983a, *Aerosol exchange between atmosphere and sea*, Stud. i Mater. Oceanol., 50, 10–18.

Garbalewski C., 1983b, *Mean spatial distribution of basic physical characteristics and source regions of particle emission from the ocean surface*, Oceanologia, 14, 139–165.

Large W. G., Pond S., 1982, *Sensible and latent heat flux measurements over the ocean*, J. Phys. Oceanol., 12, 464–482, (in Polish).

Marks R., 1987, *Marine aerosols and whitecaps in the North Atlantic and Greenland Sea Regions*, Deutsch. Hydrogr. Z., 40, 2–8.

Marks R., Monahan E. C., 1988, *Relationships between marine aerosols. Oceanic whitecaps and low-elevation winds observed during the HEXMAX Experiment in the North Sea*, Connecticut Sea Grant College Program, Groton CT.

Mestayer P. G., 1990, *Enhancement of sea to air-moisture flux by spray-droplets associated with breaking waves and bubble entrainment: Emulations in IMST wind-wave tunnel*, Hexos Contributions, 22, University of Connecticut, Point Groton.

Piskozub J., 1991, *A monostatic, multisystem lidar in studies of the marine aerosol – a solution to an inverse problem*, Ph. D. thesis, University of Gdańsk, Gdańsk, (in Polish).

Potter J., 1987, *Two-frequency lidar inversion technique*, Appl. Opt., 26, 1250–1256.

Robakiewicz M., 1991, *The analysis of the long-term variability in extreme wave conditions in the region of the Hel Peninsula in the southern Baltic*, Ph. D. thesis, University of Gdańsk, Gdańsk, (in Polish).

Thurman H. V., 1982, *An outline of oceanology*, Wyd. Mor., Gdańsk, (in Polish).

Zieliński T., Korzeniewski K., Falkowska L., 1992, *Preliminary application of lidar to measurements of the marine aerosol concentration in the atmosphere over the Gulf of Gdańsk at Sopot*, Oceanologia, 33, 191–201.

Zuyev V. E., Naats J. E., 1983, *Inverse problems of lidar sensing of the atmosphere*, Springer Verlag, Berlin.